ELSEVIER

Thermochimica Acta 304/305 (1997) 157–163

thermochimica acta

Some aspects of recent improvements of temperature-modulated calorimeter

Kenji Ema*, Haruhiko Yao

Department of Physics, Faculty of Science, Tokyo Institute of Technology, 2-12-1 Oh-okayama, Meguro, Tokyo, 152, Japan

Received 20 July 1996; accepted 14 March 1997

Abstract

Some aspects of recent improvements in temperature modulated calorimeter have been described. The contents are: (1) a low-frequency AC calorimeter with an improved resolution; $\delta C_p/C_p \cong 0.010\%$, $\delta T \sim 7\,\mathrm{mK}$; (2) an ultra-low frequency fully automated multifrequency AC calorimeter operated down to 0.5 mHz; and (3) a calorimeter with a capability of both AC-mode and relaxation-mode operations. © 1997 Elsevier Science B.V.

Keywords: AC calorimetry; Heat-capacity spectroscopy; Relaxation calorimetry; Temperature-modulated calorimetry

1. Introduction

A variety of temperature-modulated calorimetric methods have been developed in the past, including the AC calorimetry, relaxation calorimetry, and dynamic DSC, etc. Most of these calorimeters have an advantage of yielding a high resolution [1] relatively easily with only a small amount of sample. AC calorimetry is the most significant among them. In this paper, we describe examples of our recent improvements in AC calorimetry and some related techniques which have been used in our study on liquid crystals and lipid-membrane systems. The principle of AC calorimetry as well as the derivation of basic equations needed for its data analysis were described by Sullivan and Seidel [2], and also by other authors [3]. Therefore, we present here only a rather simplified description of the experimental method. In Section 3, our high-resolution AC calorimeter has been described. Then, in Section 4, an ultra-low frequency fully automated multifrequency AC calorimeter is described. Section 5 describes a calorimeter with a capability of both AC-mode and relaxation-mode operations.

2. Basic principle of AC calorimetry

In an AC calorimeter, a sample is loosely linked to a heat bath. In Fig. 1(a), the thermal link is represented by a thermal resistance R. An AC heat input $P_{AC}\exp(i\omega t)$ is supplied to the sample. The AC heat input to the sample causes the temperature of the sample to oscillate with a frequency equal to the heat input. Fig. 1(b) shows an electrical equivalent circuit. The current source P_{AC} corresponds to the AC heat input of the sample, and the capacitor C corresponds to the heat capacity of the sample. The voltage across the capacitor corresponds to the temperature difference between the sample and the bath. The angular frequency ω of heating has been chosen so that the thermal relaxation time τ_D is much smaller than the heating period, i.e. $\omega\tau_D \ll 1$. This condition means

*Corresponding author.

PII S0040-6031(97)00179-2

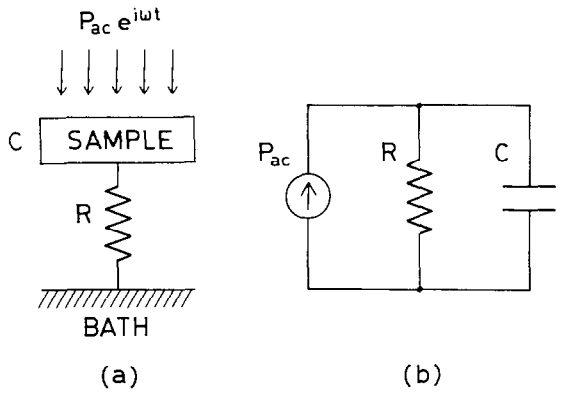

Fig. 1. The thermal system in (a) – the present calorimeter, and (b) – its electrical equivalent circuit.

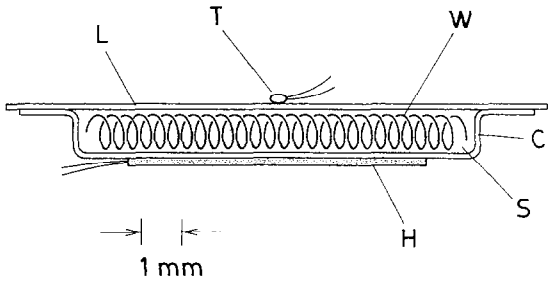

Fig. 2. Sample cell [6]. S – sample; C – gold cup; L – gold lid; W – gold wire; H – heater; and T – thermistor.

that the temperature oscillation is slow enough so that the temperature gradient over the sample is negligibly small. Because of this condition, the sample can be described as a single capacitor as in Fig. 1(b). Otherwise, the sample should be treated as a distributed constant circuit reflecting the thermal diffusion inside the sample. The amplitude T_{AC} of the sample temperature oscillation is given as

$$T_{AC} = \frac{P_{AC}}{R^{-1} + i\omega C}, \tag{1}$$

where P_{AC} is the amplitude of the AC heat input [4]. In a usual AC calorimeter, the heating frequency is chosen so that the first term in the denominator of the right-hand side of Eq. (1) is negligible in comparison with the second, i.e.

$$\omega RC \gg 1. \tag{2}$$

This condition, called the adiabatic condition, determines the lower frequency limit of the measurement. Using the condition (2), Eq. (1) simplifies to

$$T_{AC} \cong -i\frac{P_{AC}}{\omega C}. \tag{3}$$

The prefactor $-i$ indicates that the phase of T_{AC} is delayed by $\pi/2$ from P_{AC}.

3. Improvement in precision

The main advantage of the AC method is its high precision. We have concentrated our efforts to extend this merit as far as possible. At present, our calorimeter enables us to obtain heat capacity data with a precision of $\delta C/C \sim 0.010\%$ (this value quotes the standard error in the total heat capacity, including the sample cell) with a temperature resolution of ca. 7 mK [5].

Fig. 2 shows the cell design used in our calorimeter [6]. A sample of (30–50) mg is put into a gold cup 13 mm in diameter and ca. 1 mm deep pressed from 0.25 mm foil. A gold lid, 0.2 mm in thickness, is pressed onto the lip of the gold cup without any precoating. In the case of liquid crystal samples, helium gas is filled in the cell to avoid the thermal deterioration of the sample during the measurement. The cell is heated with a thin plate heater (strain gauge, type KFD-5C1-11, Kyowa Electric Instruments) attached on the bottom surface of the cell with a thin coat of GE7031 varnish. The temperature of the cell is detected by a small-bead thermistor, ca. 0.3 mm in diameter (VECO 0.013" Small Beads, Victory Engineering, or Series 111, Fenwal Electronics), attached on the opposite surface of the cell. Gold wire, 0.15 mm in diameter and ca. 400 mm in length is wound in the shape of a coil 0.8 mm in diameter and ca. 50 mm in length. This coil is formed into a spiral, and put into the cell. This gold wire greatly reduces the effective thermal relaxation time τ_D mentioned in the previous section, especially when a relatively large amount of liquid sample is used. In most measurements on liquid crystal samples, however, the gold wire is not used. In that case, the sample forms a very thin layer at the bottom of the cup, resulting in a small enough τ_D (notice that τ_D is proportional to the square of layer thickness [2]).

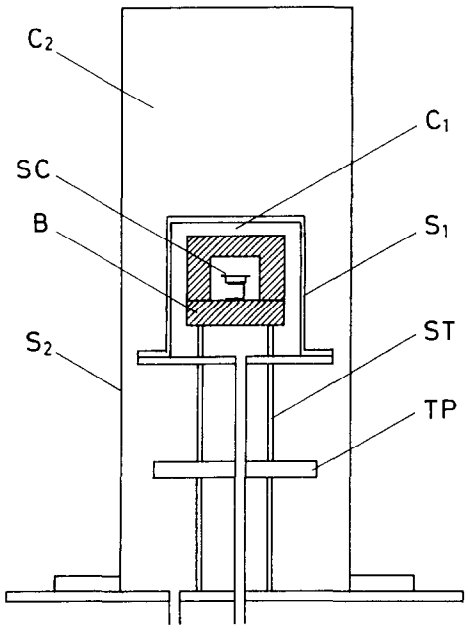

Fig. 3. The schematical view of the calorimeter. SC – sample cell; B – thermal bath (copper); S_1 – inner shield (brass, heater is wound around it); S_2 – outer shield (stainless); C_1 – inner chamber; C_2 – outer chamber; ST – stainless stem; and TP – Teflon plate.

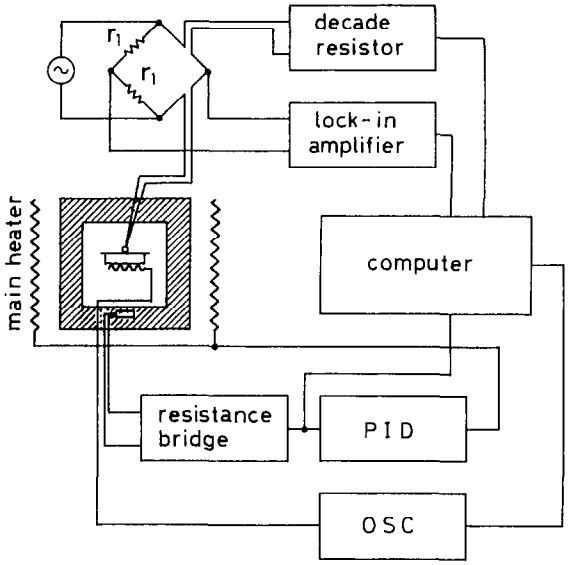

Fig. 4. Block diagram of the calorimeter.

Fig. 3 shows a schematic view of the apparatus. The thermal bath B is a cylindrical copper block 60 mm in diameter and 55 mm in height. It has an inner space of 30 mm in diameter and 25 mm in height, in which the sample cell SC is placed. A pair of copper-wire leads coated with polyimide 0.35 mm in diameter and ca. 30 mm in length are used to support the cell. The thermal link between the cell and the bath is provided in part by these wires and in part by the nitrogen gas of 1 atm surrounding the cell. The temperature of the bath can be controlled by the heater wound around the inner shield S_1. The inner chamber C_1 and the outer chamber C_2 can be pumped separately.

Fig. 4 shows the block-diagram of the calorimeter. A programmable 16-bit DA converter with a temperature coefficient of $\pm 0.005\%$ max. is used as the signal-source oscillator for the AC heating. Usually, the heating frequency is 0.03125 Hz, and the heating power 0.5 mW. This AC heating causes the AC temperature response of typically 7 mK(rms), which determines the temperature resolution of the measurement. The thermistor for monitoring the sample temperature comprises one arm of a Wheatstone bridge, which balances when the resistance of the thermistor is equal to that of a remote-control six digit variable resistor. This variable resistor is composed of metal-foil precision resistors with temperature coefficient of $< \pm 3$ ppm/K (Alpha Electronics MB and MC series). The same type of resistors are used as r_1 ($= 1\ \mathrm{k}\Omega$ in the present apparatus) in the Wheatstone bridge. The Wheatstone bridge is driven at 11.5 Hz using HP33120A function generator as the signal source. The imbalance signal of the bridge is fed into a lock-in amplifier (Seiko EG&G 5209). The output of the lock-in amplifier is read with a 5.5-digit digital multimeter, synchronized with the AC heating over six heating cycles. Usually, 768 readings are collected in this process, and the data are Fourier-transformed in a personal computer. To obtain a high stability over a long period, it is necessary in most cases to monitor the overall sensitivity of the bridge, which is affected by the drift of the oscillator output, and that of the sensitivity of the lock-in amplifier. To do this, the setting of the six-digit resistor is changed by a certain amount, and the change in the output of the lock-in amplifier is measured. This procedure is carried out after each reading process described above. The amplitude of the signal source for the Wheatstone bridge is adjusted so that the power dissipation in the thermistor does not exceed ca. 30 μW. To obtain the

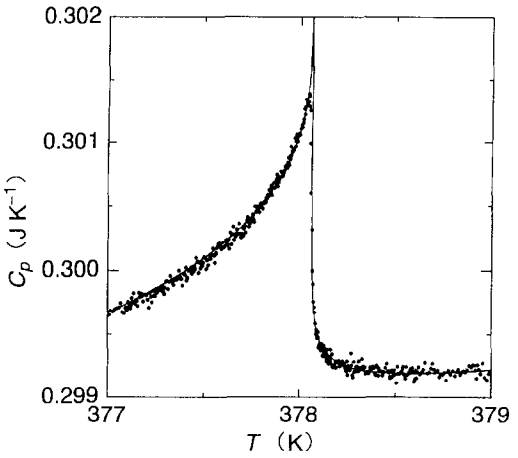

Fig. 5. Heat capacity of MHPOCBC near the smectic-*A*–smectic-C_α^* transition. The heat capacity of the gold cell is included in the data.

highest signal-to-noise ratio, the thermistor resistance should be between 2 and 20 kΩ. The temperature of the bath is detected with a platinum resistor thermometer (Okazaki Seisakusho, 1620/1), and read with an automatic resistance bridge (ASL F17A). The platinum resistor has been calibrated with an accuracy [1] of 0.1 K. Usually, the bath temperature is scanned with a rate of 1 mK/min near the transition temperature. If needed, it is also possible to keep the bath temperature constant with a stability of 0.1 mK. At present, the calorimeter can be operated in the (−10–240)°C temperature range.

Fig. 5 shows an example of the heat capacity data. A sample cell which contained 45.7 mg of antiferroelectric liquid crystal methylheptyloxycarbonylphenyl octyloxycarbonylbiphenyl carboxylate (MHPOCBC) was used. The peak at ca. 378 K is due to the smectic-*A*–smectic-C_α^* transition. The standard deviation of the scatter of the data points is 3.0×10^{-5} J/K, which is 0.010% of the total heat capacity [7].

4. Towards lower frequency: A fully automated multifrequency AC calorimeter

AC calorimetry measures the dynamic heat capacity. Therefore, we can obtain information of the internal relaxation process which couples with the entropy of the system by studying the frequency dependence of the dynamic heat capacity. Such a technique is known as heat-capacity spectroscopy [8,9]. In this technique, the frequency range covered by the measurement should be as wide as possible. In some cases the relaxation process to be studied is quite slow, which necessitates going to a lower frequency. In our recent study on the multilamellar vesicles of phosphatidylcholines, it was found that the characteristic relaxation time is more than 100 s, and we extended the lower limit of our measurement to 0.5 mHz for this purpose in the way described below [10]. This calorimeter can be operated fully automatically at preprogrammed frequencies.

The lower limit of the AC calorimeter is usually determined by the adiabatic condition (2) mentioned in Section 2. However, we choose to use Eq. (1) without using the condition (2). To do so, the value of the thermal link R should be known. We estimated the value of R from the relaxation-mode operation using the same sample settings. The details of the relaxation-mode measurement will be given in the next section.

In the presence of an appreciable internal relaxation, the heat capacity becomes complex, and can be written as

$$C = C'(\omega) - iC''(\omega), \tag{4}$$

where the real part $C'(\omega)$ and the imaginary part $C''(\omega)$ are both dependent on ω. Substituting Eq. (4) into Eq. (1), the absolute value of T_{AC}, denoted as $|T_{AC}|$, and the phase of T_{AC} in comparison with P_{AC}, denoted as ϕ, are expressed as

$$|T_{AC}| = \frac{|P_{AC}|}{\omega C'(\omega)} \left\{ 1 + \left[\frac{1}{\omega C'(\omega) R} + \frac{C''(\omega)}{C'(\omega)} \right]^2 \right\}^{-1/2}, \tag{5}$$

$$\phi = -\frac{\pi}{2} + \arctan\left[\frac{1}{\omega C'(\omega) R} + \frac{C''(\omega)}{C'(\omega)} \right]. \tag{6}$$

Solving for $C''(\omega)$ and $C''(\omega)$, we obtain

$$C'(\omega) = -\frac{|P_{AC}|}{\omega |T_{AC}|} \sin\phi, \tag{7}$$

$$C''(\omega) = \frac{|P_{AC}|}{\omega |T_{AC}|} \cos\phi - \frac{1}{\omega R}. \tag{8}$$

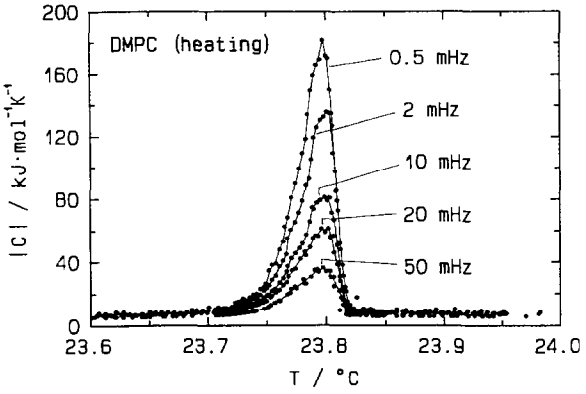

Fig. 6. Absolute value of the dynamic heat capacity of DMPC multilamellar vesicles [10].

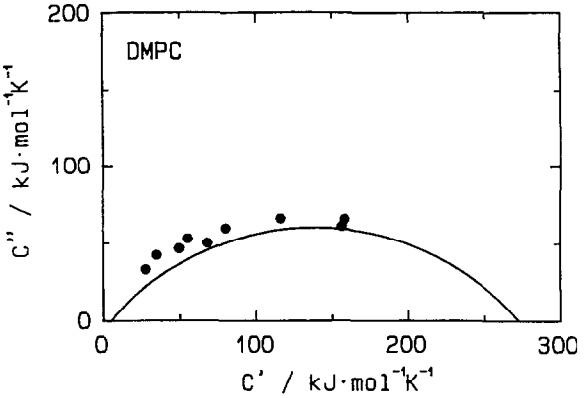

Fig. 7. Cole–Cole plot of the dynamic heat capacity obtained at the temperature of heat capacity peak of DMPC [10].

This ultra-low frequency AC calorimeter can be operated fully automatically at a series of preprogrammed frequencies. The overall design of the calorimeter is basically the same as that described in the previous section. The bath temperature is changed stepwise, each step being 3 mK in the vicinity of the transition temperature, and measurement is made after the bath temperature is stabilized within ±0.15 mK. At each temperature, measurements at programmed frequencies (usually nine frequencies ranging from 0.5 to 50 mHz) are made. The entire measurement procedure at each temperature needs ca. 5 h.

Fig. 6 shows the absolute value of the dynamic heat capacity of multilamellar vesicles of dimyristoylphosphatidylcholine (DMPC) [10]. The peak at ca. 23.8°C is attributed to the main transition. The peak-height depends significantly on the measuring frequency, indicating a very slow relaxation nature of this transition. Fig. 7 shows a Cole–Cole diagram of the complex heat capacity obtained at a temperature which gives the maximum heat capacity. The arc in the figure is a fit to the data with the following formula [11]:

$$C(\omega) = C_\infty + \frac{C_0 - C_\infty}{1 + (i\omega\tau)^\beta}. \quad (9)$$

The relaxation time τ for this fit is 119 s. It is seen in the figure that the present frequency region covers only the upper half of the dispersion curve. Further efforts to extend the lower limit of the measuring frequency is still in progress.

5. Calorimeter with both relaxation-mode and AC-mode operations

It is a serious drawback of the AC method that the estimation of the latent heat at the first-order phase transition is difficult. On the other hand, the relaxation method allows us a moderately accurate [1] estimation of the latent heat although the precision [1] of the measurement is not high as in the AC method. Such a situation has motivated us to construct a calorimeter with the capability of both an AC-mode and a relaxation-mode operation [6]. The most significant advantage of this calorimeter is that the relaxation-mode measurement provides an acceptably accurate estimation of the latent heat, while the AC-mode measurement provides rather precise heat capacity data. Further, this calorimeter can be operated in both modes using the same sample cell and the same apparatus setting.

The overall structure of the calorimeter is basically the same as described in Section 3, and the AC-mode operation proceeds in a similar way. In the relaxation mode, the power input to the sample, denoted as P, is a step function of time t. In the 'heat regime', P is switched at time $t = 0$ from 0 to a certain constant value P_0, and in the 'cool regime', from P_0 to 0. This

heat input results in an exponential relaxation of the sample temperature [12]:

$$T(t) = T_B + T_\infty(1 - e^{-t/\tau_1}) \quad (10)$$

for the heat regime, and

$$T(t) = T_B + T_\infty(e^{-t/\tau_1}) \quad (11)$$

for the cool regime. Here T_B is the temperature of the bath, $T_\infty = RP_0$, and $\tau_1 = RC$. Typically, $P_0 \cong 1.2\,\text{mW}$, and $T_\infty \cong 0.12\,\text{K}$. Prior to the relaxation-mode measurement, the bath temperature is stabilized within ± 0.1 mK by using a PID feedback controller. Then, a pair of heat-regime and cool-regime measurements are made. In each measurement, the temperature of the bath and the sample are read every 625 ms for 250 s after switching-on (or off) of the heater power. The temperature response is analyzed with Eq. (10) or Eq. (11), which gives τ_1 and T_∞, and the values of C and R are obtained therefrom. Following this, the setting of the bath temperature is changed for the next measurement. The measurement cycle is repeated usually every 40 min.

In obtaining Eqs. (10) and (11), it has been assumed that the temperature dependence of the heat capacity C over the interval T_∞ is negligibly small. This assumption is valid in most cases for the relatively small T_∞ mentioned here. A possible origin that may cause the response of the sample temperature to deviate from the simple exponential behavior as Eq. (10) or Eq. (11) is the so-called τ_2 effect [12]. The τ_2 effect can be neglected when τ_2 is much smaller than τ_1, as in the present case ($\tau_1 \sim 30$–40 s, $\tau_2 \sim 1$ s). Fig. 8 is an example of the measured temperature response of the sample in the present apparatus. Here, the difference of the sample temperature $T(t)$ from the value attained after a sufficiently long time, $T(\infty)$, has been plotted in a semi-logarithmic scale. It is seen that the deviation from the simple exponential behavior is negligible.

Another example where the response of the sample temperature deviates from the simple exponential behavior is seen at the first-order phase-transition temperature. In such cases, the deviation from the exponential response is sensitively detected by calculating the time-dependent heat capacity $C(t) \equiv \dot{Q}/\dot{T}$, where $\dot{Q}$ is the instantaneous heat flow into the sample

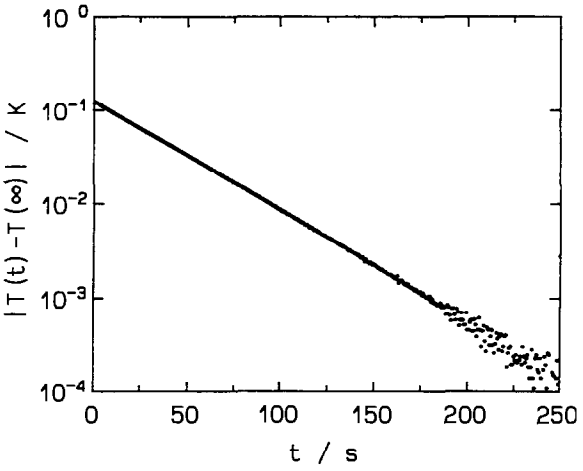

Fig. 8. An example of the response of the sample temperature in relaxation-mode measurement [6].

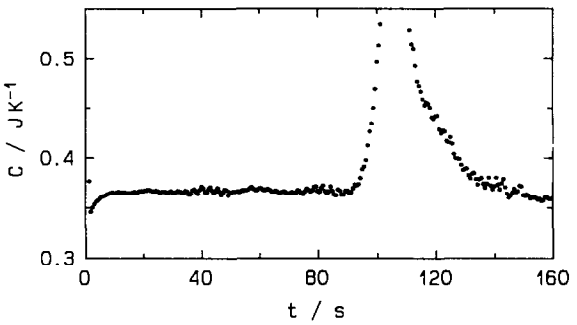

Fig. 9. The time-dependent heat capacity obtained on MHPOBC near the smectic-C^*–smectic-C^*_α transition [6].

and, therefore,

$$\dot{Q} = P_0 - \frac{1}{R}(T - T_B), \quad (12)$$

and $\dot{T} \equiv dT/dt$. Fig. 9 shows an example of the time-dependent heat capacity calculated from the data obtained on antiferroelectric liquid-crystal methylheptyloxycarbonylphenyl octyloxybiphenyl carboxylate (MHPOBC) [6,13]. The value of the latent heat L is obtained by integrating the excess heat absorption $\dot{Q}^{\text{anom}}$:

$$\dot{Q}^{\text{anom}} = \dot{Q}(t) - \dot{Q}_0. \quad (13)$$

Here, $\dot{Q}_0$ is the heat absorption due to the normal heat

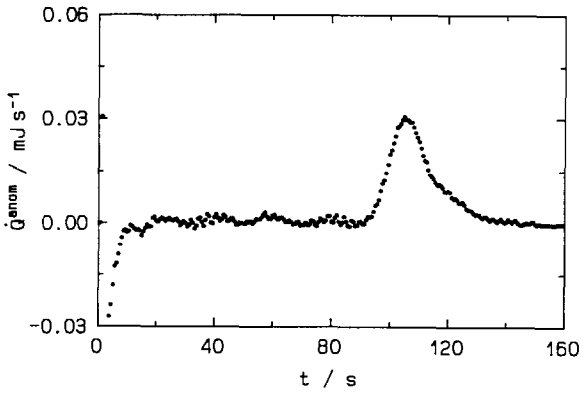

Fig. 10. Plot of excess heat absorption obtained from the data shown in Fig. 9 [6].

capacity, and is given as

$$\dot{Q}_0 = C_0\dot{T}(t), \tag{14}$$

where C_0 is the normal time-independent value of the heat capacity, which is determined as the plateau value of $C(t)$ away from the peak. Thus, we have

$$L = \int_0^\infty \dot{Q}^{\text{anom}}\,\mathrm{d}t \tag{15}$$

$$= \int_0^\infty [C(t) - C_0]\dot{T}(t)\mathrm{d}t. \tag{16}$$

Fig. 10 shows a plot of $\dot{Q}^{\text{anom}}$ against t calculated for the data shown in Fig. 9. The latent heat is obtained by integrating the anomaly seen in this figure, and dividing it by the sample weight $m = 31.4$ mg. The latent heat obtained in this way for nine data sets when the $\mathrm{Sm\,C^*} - \mathrm{Sm\,C^*_\alpha}$ transition was observed, agreed with each other rather well and had a value of $0.021\,\mathrm{J/g} = 12\,\mathrm{J/mol}\ \pm 10\%$.

Recently, one of the present authors (H. Yao) has developed a new type of relaxation method in which the heater power is linearly ramped. For a heating run, $P = 0$ for $t < 0$, $P = \dot{P}t$ for $0 \le t \le t_1$ where $\dot{P}$ is a constant, and $P = P_0 = \dot{P}t_1$ for $t_1 < t$. The details of this method will be described elsewhere [14].

Acknowledgements

The authors wish to thank Professor C.W. Garland for helpful discussions. Acknowledgment is also made to the publishers of the journals for permission to use the figures.

References

[1] Throughout this paper we use 'resolution' or 'precision' to describe the error in the relative values, and 'accuracy' to describe the error in the absolute values obtained in the measurement.
[2] P. Sullivan and G. Seidel, Phys. Rev., 173 (1968) 679.
[3] See, for example, C.W. Garland, Thermochim, Acta, 88 (1985) 127; I. Hatta and A. Ikushima, Jpn. J. App. Phys., 20 (1981) 1995 and references therein.
[4] In some cases a square wave is used as the AC heat input, Then the amplitudes of the fundamental components can be used for T_{AC} and P_{AC}.
[5] K. Ema, J. Watanabe, A. Takagi and H. Yao, Phys. Rev. E, 52 (1995) 1216.
[6] K. Ema, T. Uematsu, A. Sugata and H. Yao, Jpn. J. Appl. Phys., 32 (1993) 1846.
[7] The 'total' heat capacity means that the heat capacity of the gold cell is included. The relative resolution in the sample heat capacity depends on the amount of the sample contained in the cell. In the case shown here, about one third of the total heat capacity is the sample heat capacity.
[8] N.O. Birge, Phys. Rev. B, 34 (1986) 1631.
[9] T. Christensen, J. Phys. (Paris) Colloq., 46 (1985) C8 635.
[10] H. Yao, H. Nagano, Y. Kawase and K. Ema, Biochim, Biophys, Acta, 1212 (1994) 73.
[11] This form is widely accepted for analyzing the dielectric dispersion data, See K.S. Cole and R.H. Cole, J. Chem. Phys., 9 (1941) 341; Also see, for instance, B.K.P. Scaife, Principles of Dielectrics, Oxford University Press, Oxford, 1989, p. 67.
[12] R. Bachmann and F.J. DiSalvo Jr.T.H. Gevalle, R.L. Greene, R.E. Howard, C.N. King, H.C. Kirsch, K.N. Lee, R.E. Schwall, H.-U. Thomas and R.B. Zubeck, Rec. Sci. Instrum., 43 (1972) 205.
[13] K. Ema, H. Yao, I. Kawamura, T. Chan and C.W. Garland, Phys. Rev. E., 47 (1993) 1203.
[14] H. Yao and C.W. Garland (in preparation).